The Journal of the Acoustical Society of America

SEPTEMBER 27 2007

High frequency broad band scattering from water-saturated granular sediments: Scaling effects

Anatoliy N. Ivakin; Jean-Pierre Sessarego

J. Acoust. Soc. Am. 122, EL165–EL171 (2007)
https://doi.org/10.1121/1.2784534

ASA
ACOUSTICAL SOCIETY OF AMERICA

High frequency broad band scattering from water-saturated granular sediments: Scaling effects

Anatoliy N. Ivakin
Applied Physics Laboratory, University of Washington, Seattle, Washington 98105
ivakin@apl.washington.edu

Jean-Pierre Sessarego
CNRS/LMA, 31 Chemin Joseph Aiguier, 13402, Marseille, Cedex 20, France
sessarego@lma.cnrs-mrs.fr

Abstract: Sound backscattering from water-saturated granular sediments at frequencies from 150 kHz to 8 MHz at oblique incidence was studied in controlled laboratory conditions. Two kinds of sediments, medium and coarse sands, were degassed, and their surface was flattened. In these conditions, the sediment granular structure can be considered as a controlling mechanism of backscattering. Comparison of frequency dependencies of backscatter for the two sediments with different mean grain size shows the existence of a persistent scaling effect that allows description of the backscattering strength as a function of one parameter, the mean grain size/wavelength ratio.

PACS numbers: 43.30.Ma [GD]
Date Received: June 3, 2007 **Date Accepted:** August 23, 2007

1. Introduction

Reported measurements of seabed scattering are largely confined to relatively low frequencies, up to 300 kHz (see, e.g., Jackson and Richardson[1] and references therein). Still higher frequencies, up to a few megahertz, are used in seafloor imagery (e.g., in pencil-beam sonars), particularly to observe dynamic processes at the seafloor. From the physics of sound-sediment interaction standpoint, however, interesting effects can be anticipated at these high frequencies as the wavelength can become comparable with the sediment typical grain sizes. Unfortunately, existing observations in this case are usually noncalibrated and, therefore, do not allow measurements of system independent scattering characteristics of the seabed, such as the bottom scattering strength. A recent exception is presented in Greenlaw *et al.*,[2] where the backscattering strength for sand sediments in shallow water was measured at frequencies from 265 kHz to 1.85 MHz. However, physical interpretation of results obtained in this work is quite ambiguous due to a significant uncertainty of the sediment parameters. As the authors noted,[2] the sediment surface was only relatively smooth and had, e.g., pockmarks created by fish foraging on the bottom fauna. A small but detectable sediment gas content was noticed as well. Therefore, acoustic observations could be affected by the small-scale roughness, the presence of gas bubbles in the sediment, and other mechanisms, e.g., those related to possible near-surface stratification of the sediment.[3,4]

Unfortunately such ambiguities are quite usual for experimental studies of sediment acoustics in shallow water where the dynamical complexity and unpredictability of environmental conditions can be so great that even very extensive time- and labor-consuming environmental measurements (such as those at the recent major sediment acoustics experiment, SAX04[5,6]) may not be enough to sufficiently reduce the uncertainty in interpretation of acoustic data. In this connection, conducting experiments in well-controlled laboratory conditions can become a valuable (but much less expensive) supplement to the experiments at sea. An impor-

tant advantage of laboratory studies of sediment scattering is that they make it possible to simplify the problem by reduction of the number of controlling parameters and allow observation of the effects of different scattering mechanisms separately. For example, the sediment can be degassed to eliminate effects of micro-bubbles, and its surface can be flattened to exclude contributions of the sediment roughness at scales greater than the grain size. This approach was used by Nolle *et al.*[7] in their study of acoustical properties of sand sediments at two frequencies, 500 kHz and 1050 kHz. Williams *et al.*[8] studied broadband backscattering from several types of the sediments in a wider frequency range, about 200 kHz to 2.5 MHz. Unfortunately, the bottom scattering strength was not obtained, as the measurements were still not calibrated.

In this paper (Sec. 2), we describe experiments conducted at the CNRS/LMA water tank facility on backscatter from sands over a wide frequency range, 150 kHz to 8 MHz. Note that existing methods for measuring the bottom scattering strength normally assume using narrow band signals (see, e.g., Jackson and Richardson,[1] Ch. G.2, pp. 497–502). To be applied to broadband transducers, significant modifications are required. One such modification is considered in Sec. 3 of this paper. It made possible, to our knowledge for the first time, measurement and analysis of the frequency dependence of the sediment backscattering strength over such a wide frequency range. The results are given in Sec. 4. The analysis assumes that, for the given conditions, only one mechanism of scattering can be dominating, which is due to the sediment granular structure, and that the controlling sediment parameter is the mean grain size. In this case a scaling effect is possible: Given grazing angle, the backscattering strength, which is system independent and depends only on frequency and sediment properties, can be presented as a unique function of only one parameter, the mean grain size/wavelength ratio. This effect is demonstrated and the scaling function is presented in Sec. 4 as well.

2. Experiments

Two kinds of water-saturated sediments with different grain sizes, moderately well sorted medium and coarse sands, were chosen for the study. Sediment properties such as the density, porosity, and grain size, were measured by nonacoustical methods. The medium sand had the mean grain diameter 0.245 mm, sediment/water density ratio 1.98, and porosity 36.5%. The coarse sand had the mean grain diameter 1.55 mm, sediment/water density ratio 2.02, and porosity 33%. Prior to the experiments, the two sediments were stored in containers filled with water treated with chlorine to exclude the presence of living organisms which might generate bubbles. The sediments were transferred in smaller containers (without exposure to air) to a large water tank (chlorine treated as well) where, in addition, they were sieved and agitated to eliminate remaining bubbles. After such preparations, the two sediments were placed in different plastic rectangular boxes of the same size with horizontal dimensions 17×23 cm and 9 cm in the vertical. The sediment surface was carefully flattened by scraping even with the box edges to eliminate roughness at scales larger than the sediment grains. Therefore, the necessary measures were taken to ensure that only the sediment granular structure be considered as a dominating mechanism (rather than large scale roughness and/or gas bubbles) controlling total scattering in and from the sediment.

Experiments on backscattering from the sediments were conducted using a typical monostatic geometry with the transducers acting as both source and receiver (see, e.g., Jackson and Richardson,[1] Fig. G3). Two broadband Parametrics transducers with nominal center frequencies 500 kHz and 5 MHz were used which, altogether, allowed covering continuously the wide frequency range of 150 kHz to 8 MHz. The transducers are circular pistons with radii 12.5 mm (500 kHz) and 6.5 mm (5 MHz). Their directivities are documented over all used frequencies and well described by the corresponding theoretical function $D=2J_1(ka \sin \vartheta)/(ka \sin \vartheta)$, where a is the piston radius, $k=2\pi/\lambda$ is the wave number in water, $J_1(\ldots)$ is the Bessel function of the first order, and ϑ is the angle between the direction of observation and the maximum response axis (MRA) of the transducer.

The position of the transducers was controlled by a system allowing their automatic vertical and horizontal translation with 0.1 mm accuracy and their rotation with 0.1° accuracy.

For calibration of each transducer, first the time series of the echo signal reflected from the water-air interface at normal incidence were measured and Fourier analyzed. Then, the transducer was rotated toward the sediment surface and set in a position with a fixed direction. Horizontal translations of the transducer (parallel to the sediment surface) were used to develop a statistically uniform ensemble of realizations for the echo signals. To provide the necessary statistics, a number of horizontal positions of the transducer was set automatically with a consecutive horizontal shift of 0.5 cm. At each position, time series of the echo signal scattered from the sediment (at a fixed incidence angle) were measured for a number of pings (up to 64) and coherently averaged to reduce possible effects of noise.

Fourier spectral analysis was performed on the echo signals with a flexible time-windowing. The windowing was used, first, to reduce the effects of reverberation from the sediment box walls and, second, to accommodate corresponding distances and the scattering areas of the sediment surface with the frequency dependent beam pattern of the transducer (as discussed below). The windowed echo frequency spectra, $F(f)$, were normalized by the spectra of the calibration signal, $F_0(f)$. These normalized spectra provided a data set for the statistical processing. Particularly, their second moments (the squared magnitudes averaged over realizations), were used to estimate the normalized scattered intensity

$$I_s(f)/I_0(f) = \langle |F(f)|^2 \rangle / |F_0(f)|^2, \tag{1}$$

and to obtain the frequency dependencies of the sediment backscattering coefficient, m_s, and its decibel equivalent, the scattering strength, 10 log m_s, as given in the next section.

3. Extracting scattering strength

The intensity of calibration and scattered signals in the frequency domain, I_o and I_s [see Eq. (1)], can be calculated from the corresponding signal time series taken in the observation time window. Specifically, the scattering intensity is defined as the squared magnitude of the Fourier transform of the scattered signal time series taken in the time window, $t \in [t_1, t_2]$, related to time-delays occurring in the process of scattering and defined by corresponding range-time inequality

$$ct_1 < r_i + r_s < ct_2, \tag{2}$$

with r_i and r_s being the distances from the source and receiver to the ensonified area (or, more accurately, the observation area) and c being the sound speed in water.

Consider the case of a monostatic geometry, where $r_i = r_s = r = ct/2$. The incidence angle (measured from the vertical), θ, is defined as follows: $\cos\theta = t_f/t$, $t \geqslant t_f = 2H/c$, where t_f is the arrival time in the vertical direction (fathometer return) and H is the vertical distance from the source to the sediment surface. For the angle window $\theta \in [\theta_1, \theta_2]$, taking into account that $\tan\theta d\theta = d \ln t$, we have $\theta_2 - \theta_1 \approx (t_2 - t_1)/t_w \tan\theta_w$ with $t_w = (t_1 + t_2)/2$ and $\theta_w = (\theta_2 + \theta_1)/2$ being centers of the corresponding time and angle windows.

The scattering cross section per unit area per unit solid angle (see, e.g., Ref. 1, p. 23) or, for brevity, the scattering coefficient, m_s, can be defined from the equation

$$I_s = I_o \frac{r_o^2}{r^4} A_{ef} m_s, \tag{3}$$

where I_o is the intensity at the distance $r_0 = ct_0$ in the direction of maximum directivity (on the transducer MRA) with t_0 being the arrival time of the calibration signal, and A_{ef} is an effective observed scattering surface obtained from the directivity D, defined with respect to the field amplitude, by integration over the observation area, defined by Eq. (2), as follows:

$$A_{ef} = \int_{A(t)} D^4 dA. \tag{4}$$

The integral (4) can be written using spherical variables (θ, φ), which are the incidence and azimuth angles of the incident wave. However, for directional sources not vertically oriented, it is more convenient to describe their directivity and analyze the integral (4) in angular coordinates measured not from vertical direction, but from the transducer MRA, i.e., from its depression incidence angle, θ_0. Consider new variables (not spherical), $\theta' = \theta - \theta_0$ and $\varphi' = \varphi \sin\theta$, which represent angular coordinates measured in two mutually orthogonal planes so that their intersection is the transducer MRA, where $\theta' = 0$ and $\varphi' = \varphi = 0$. One of these two planes is always vertical (the incidence plane). The second is an auxiliary one perpendicular to the incidence plane and referred to as the slant azimuth plane.

Using the new variables, the integral (4) can be written in the form

$$A_{\mathrm{ef}} = \frac{r^2}{\cos\theta_w}\Omega_{\mathrm{ef}}, \tag{5}$$

where Ω_{ef} is an effective solid angle of the observation area

$$\Omega_{\mathrm{ef}} = \int_{\theta_1}^{\theta_2} d\theta \int_{-\pi\sin\theta}^{\pi\sin\theta} D^4(\theta - \theta_0, \varphi')\, d\varphi'. \tag{6}$$

Note that the integral (6) at high enough frequencies (and correspondingly narrow directivities) has a maximal value at $\theta_w = \theta_0$, where the observation angle window matches with the maximum of the transducer directivity.

Assume that the transducer has directivity with an axial symmetry, so that for the directivity factor we have $D^4(\theta', \varphi') = Q(\vartheta/\vartheta_o)$, where ϑ is the angle between the direction of observation and the transducer MRA, and ϑ_0 is a parameter defining the directivity angular width. Note that at $\vartheta_0 \ll \theta$, limits in the φ'-integral in Eq. (6) can be replaced by infinities, and integration can be performed using an approximation $\vartheta \approx (\theta'^2 + \varphi'^2)^{1/2}$. Then, in the matching case, $\theta_w = \theta_0$, we obtain

$$\Omega_{\mathrm{ef}} \approx \vartheta_0^2 P\left(\frac{\theta_2 - \theta_1}{2\vartheta_0}\right), \quad P(\alpha) = \int_{-\alpha}^{\alpha} dx \int_{-\infty}^{\infty} Q(\sqrt{x^2 + y^2})\, dy. \tag{7}$$

The integral in Eq. (7) has two simple asymptotic approximations:

$$P \approx M_1 \alpha, \quad \alpha \ll 1, \quad M_1 = \int_{-\infty}^{\infty} Q(s)\, ds,$$

$$P \approx M_2, \quad \alpha \gg 1, \quad M_2 = 2\pi \int_0^{\infty} sQ(s)\, ds. \tag{8}$$

A uniform approximation (for arbitrary α) can be sought in the form of a scaling expression

$$P(\alpha) \approx M_2 P_\eta(\alpha M_1/M_2), \quad P_\eta(x) = (1 + x^{-\eta})^{-1/\eta}, \quad \eta > 0. \tag{9}$$

At any value of η, this approximation has two correct asymptotes [Eq. (8)] for small and large α. This allows use of η as a free parameter that can be chosen so as to provide the best fit of the scaling function [Eq. (9)] to the integral (7) at intermediate α, taking into account a specific transducer directivity function $Q(s)$.

In our case of the circular piston transducers, we can assume that at high frequencies $\vartheta_0 \equiv (ka)^{-1} \ll 1$ and perform the integration in Eqs. (7) and (8) numerically with $Q(s) = (2J_1(s)/s)^4$. For the integrals in Eq. (8) we obtain $M_1 \approx 2.4$ and $M_2 \approx 5.8 \approx M_1^2$. The result for the integration in Eq. (7) is shown in Fig. 1 by the solid curve. The uniform scaling approximation given in Eq. (9) is shown for different η by dashed curves. It is seen that the best agreement is provided by $\eta \approx 4$. Therefore, the set of Eqs. (1), (3), (5), (7), and (9) provides a practical

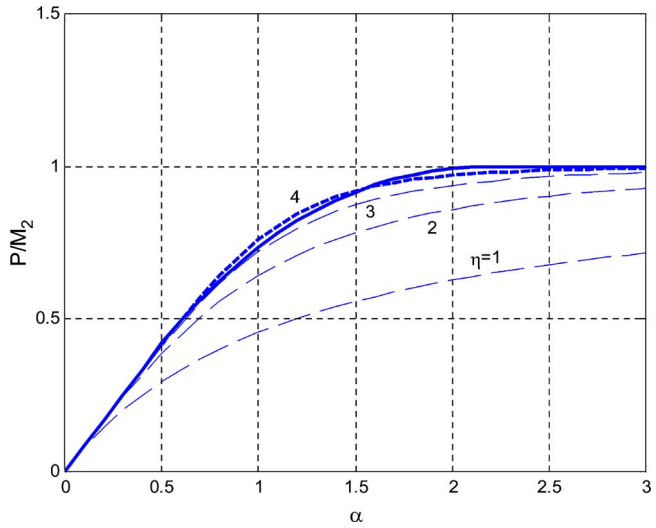

Fig. 1. (Color online) Choosing the parameter η for a scaling power law approximation (9): numerical integration for $P(\alpha)/M_2$ (solid curve) compared to the scaling function $P_\eta(\alpha M_1/M_2)$ for different η (dashed curves). The best fit is provided by $\eta \approx 4$.

algorithm for extracting the backscattering coefficient from analysis of the normalized scattered intensity in the frequency domain using time-windowing of the echo-signal.

4. Results

In Fig. 2, the frequency dependence of the backscattering strength is presented in a wide frequency range, 150 kHz to 8 MHz, for the two sediments, medium and coarse sand, at an incidence angle of 50° (grazing angle of 40°). It demonstrates, in particular, a noticeable difference in the scattering strength of the two sediments at frequencies below 2 MHz. For example, this

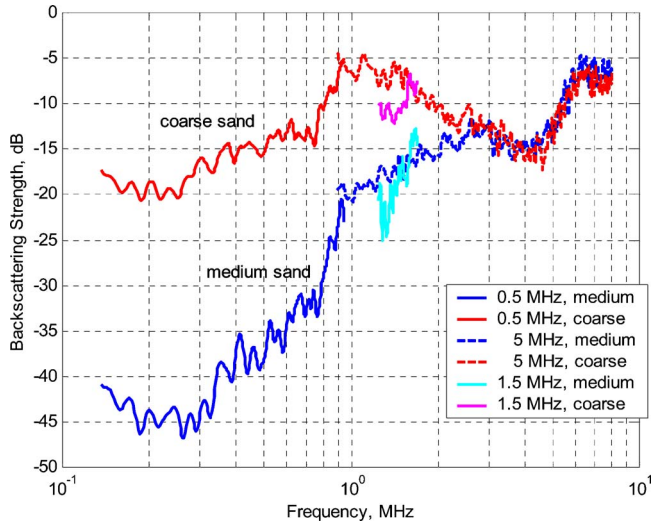

Fig. 2. (Color online) The backscattering strength at the incidence angle 50° obtained for medium and coarse sand using the broad band transducers with 500 kHz and 5 MHz nominal center frequencies. The center frequency of the 500 kHz transducer was nominal indeed, as the transducer had actually another, although weaker, maximum in its frequency spectrum, at 1.5 MHz, which was used to obtain additional scattering data.

difference at frequencies 400 kHz to 800 kHz is about 20 dB. It can mean practically important strong sensitivity of the scattering strength at these frequencies to the mean grain size of the sediment. Note also that at frequencies above 2.5 MHz the difference is small and, therefore, the scattering strength may have too little sensitivity to the grain size.

The ratio of the mean grain diameter to the acoustic wavelength in water, d/λ, varied, in our frequency range, from 0.024 to 1.3 for the medium sand, and from 0.15 to 8.3 for the coarse sand. Therefore, in the interval $0.15 < d/\lambda < 1.3$, we have two data sets for sediments with different mean grain size. This interval is especially interesting as it corresponds to a "transition frequency regime", where the acoustic properties of granular sediments can change dramatically. This change is due to transition from the "low frequency regime", where the ratio d/λ is very small and the continuum media assumptions are valid, to the "very high frequency regime", where this ratio is not small and the sediment must be considered as an essentially discrete granular medium. At these high frequencies, intrinsic (bulk) scattering due to the sediment granular structure becomes important. For example, the ratio d/λ becomes about 0.5 at frequencies around 3 MHz for the medium sand, and at 500 kHz for the coarse sand. Corresponding shift (for the sediments with different grain size) related to the "transition" effects and appearance of the new dominating scattering mechanism can be anticipated. In Fig. 2, such a scaling shift is clearly seen.

In Fig. 3, the scaling effect is demonstrated by plotting scattering data (same as in Fig. 2) versus the ratio d/λ. It is seen that the backscattering strength collapses to a function of only one parameter, at least over the interval $0.15 < d/\lambda < 1.3$, where both data sets are available. This confirms the assumption that, for the given conditions, only one mechanism of scattering is dominating, which is the intrinsic (bulk) scattering due to the sediment granular structure, and that the controlling sediment parameter is the mean grain size. In this case, the scattering strength must be a unique function of the ratio d/λ. This explains, e.g., that the two different grain-size cases match when shifted horizontally, but no shift in the vertical is needed (see Figs. 2 and 3). This is because the scattering strength is unique, system independent, and controlled only by the sediment parameters. This result is practically important, as it provides both prediction and inversion capabilities: if the scattering strength is measured at one frequency and one grain size, it can be predicted at others or inverted with respect to the grain sizes. Therefore, the scaling effects demonstrated here can potentially be used in acoustic sensing of marine sedi-

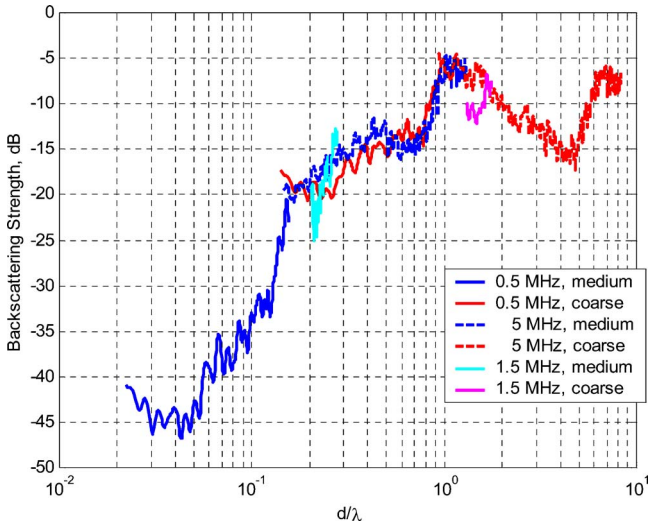

Fig. 3. (Color online) The same data as in Fig. 2, but plotted vs the sediment mean grain diameter ratio to the wavelength in water, d/λ.

ments to remotely estimate their mean grain size. Further analysis of these effects might be an interesting and promising subject of future theoretical and experimental studies.

Acknowledgments

This work was supported by the U.S. Office of Naval Research, and CNRS/LMA, France.

References and links

[1]D. R. Jackson and M. D. Richardson, *High Frequency Seafloor Acoustics* (Springer Science, New York, 2007).
[2]C. F. Greenlaw, D. V. Holliday, and D. E. McGehee, "High-frequency scattering from saturated sand sediments," J. Acoust. Soc. Am. **115**, 2818–2823 (2004).
[3]A. N. Ivakin, "High frequency scattering from sandy sediments: Roughness vs discrete inclusions," in *Boundary Influences in High Frequency Shallow Water Acoustics*, edited by N. G. Pace and P. Blondel, (University of Bath, UK, 2005), pp. 185–192.
[4]A. N. Ivakin, "Models of scattering for remote acoustic sensing of the seafloor," in *Proceedings of the Institute of Acoustics* (Bath University, Bath, UK, 2001), Vol. 23, Part 2, pp. 268–275.
[5]E. I. Thorsos, K. L. Williams, D. Tang, and S. G. Kargl, "SAX04 overview," in *Boundary Influences in High Frequency Shallow Water Acoustics*, edited by N. G. Pace and P. Blondel (University of Bath, UK, 2005), pp. 3–12.
[6]M. D. Richardson, K. B. Briggs, A. H. Reed, W. C. Vaughan, M. A. Zimmer, L. D. Bibee, and R. I. Ray, "Characterization of the environment during SAX04: Preliminary results," in *Proceedings of the International Conference on Underwater Acoustic Measurements: Technologies & Results*" (Heraklion, Crete, Greece, 28 June–1 July 2005).
[7]A. W. Nolle, W. A. Hoyer, J. F. Mifsud, W. R. Runyan, and M. B. Ward, "Acoustical properties of water-filled sands," J. Acoust. Soc. Am. **35**, 1394–1408 (1963).
[8]K. L. Williams, R. H. Hackman, and D. H. Trivett, "High-frequency scattering from liquid/porous sediment interfaces," J. Acoust. Soc. Am. **84**, 760–770 (1988).